Korean J. Chem. Eng., 40(10), 2489-2496 (2023)
DOI: 10.1007/s11814-023-1550-8

pISSN: 0256-1115
eISSN: 1975-7220

Enhanced antibiotic removal by waste coffee grounds prepared via water washing and KOH activation

Min Gyu Lee and Younghun Kim†

Department of Chemical Engineering, Kwangwoon University, Wolgye-dong, Nowon-gu, Seoul 01897, Korea
(*Received 22 June 2023 • Revised 14 July 2023 • Accepted 9 August 2023*)

Abstract−This study presents a novel approach for effectively removing amoxicillin (AMX) from waste coffee grounds (CGs) using eco-friendly activated biochar-based adsorbents. To avoid the use of toxic chemicals, the adsorbents, called ACGs (activated CGs), were prepared by a water washing method followed by KOH activation. The adsorption performance of the ACGs was evaluated using various parameters such as the Freundlich isotherm, Langmuir isotherm, adsorption density, and pseudo-second-order equation to determine their maximum adsorption capacity and kinetics. Among the ACGs tested, ACG-4a, activated with KOH after water washing, exhibited significantly higher adsorption capacity (740.7 mg/g) compared to ACG-4b, activated with KOH after NaOH washing (549.5 mg/g). The superior adsorption capacity of ACG-4a can be attributed to its specific surface area. Notably, the ACGs demonstrated the highest AMX-adsorbing capacity when compared to other adsorbents.

Keywords: Waste Coffee Ground, Amoxicillin, Adsorption, Surface Area, Water Contamination

INTRODUCTION

Contamination of common water sources with antibiotics represents a critical environmental issue [1]. The extensive utilization of antibiotics, particularly during the COVID-19 pandemic, has substantially elevated their presence in water bodies through diverse routes, including pharmaceutical manufacturing effluents, hospital wastewater, and agricultural runoff, ultimately the contamination of aquatic ecosystems [2]. The excessive usage of antibiotics carries significant implications, including the emergence and spread of antibiotic-resistant pathogens, which poses a serious threat to public health [3]. To enhance the academic context, effective strategies for the removal of antibiotics from water are urgently required.

Several methods can be employed to effectively remove antibiotics present in common water, including filtration, chemical treatment (chlorination or ozonation) [4], advanced oxidation processes [5], and adsorption [6]. Among these methods, the use of an adsorbent offers several advantages for antibiotic removal, including high adsorption capacity, selectivity, cost-effectiveness, sustainability, ease of operation, and regeneration potential. While activated carbon is commonly used as an adsorbent for antibiotic removal [7], alternative adsorbents can overcome its demerits. One such promising alternative is biochar, which is derived from the pyrolysis of organic biomass, such as wood, coconut shell, bamboo, and sewage sludge [8-10]. Owing to their cost effectiveness, sustainability, and ease of implementation, adsorbents such as coffee grounds (CGs) can be used as biochar sources to efficiently remove antibiotics from common water sources [11].

CGs are readily available waste materials generated in significant quantities worldwide. Repurposed waste CGs offer a sustainable and cost-effective feedstock for biochar production. In addition, CGs have a high carbon content, making them suitable for biochar production, which contributes to the stability and adsorption capacity of biochar [12]. The use of CGs as raw materials for biochar aligns with the principles of a circular economy. This involves repurposing waste products and converting them into valuable resources. The use of CGs as biochar for the removal of antibiotics offers a unique opportunity to simultaneously address the issues of both discarded CGs and the presence of antibiotics in water. This approach is aligned with the principles of sustainability, waste management, and environmental protection.

Washing and activation methods are typically employed to prepare waste CGs as adsorbents for the removal of antibiotics. The first step is to thoroughly wash the waste CGs to remove any organic matter or residues that may be present. It can be achieved by rinsing the CGs with water multiple times, either manually or using a filtration system. Activation is a crucial step for enhancing the surface area and adsorption capacity of CGs. Biochar activation can be achieved using both acid and alkaline activation agents: acids such as H_3PO_4 or H_2SO_4, and alkaline like KOH or K_2CO_3 [8,9]. A commonly used method is chemical activation using alkaline substances, such as KOH [13], which chemically modifies the physical structure of the biomass [14]. KOH activation is preferred due to its high reactivity, creating a porous structure with increased surface area and micropores [8]. It generates functional groups that enhance adsorption capacity and removes impurities. Compared to other agents, KOH offers superior reactivity and the ability to generate a highly porous structure with abundant functional groups [9], resulting in improved adsorption performance. Waste CGs are mixed with a solution of KOH and heated to a specific temperature to obtain activated CGs (ACG). This process creates micropores and increases the surface area [15], making waste CGs more

†To whom correspondence should be addressed.
E-mail: korea1@kw.ac.kr

effective in adsorbing antibiotics.

Therefore, in this study, we developed an optimal adsorbent capable of effectively adsorbing and removing amoxicillin (AMX), which is a representative antibiotic present in water systems. To achieve this, the efficiency of AMX removal by four waste CGs was tested using two washing methods (water and NaOH washing) and by varying the mass ratio of KOH. ACG-4a (activated by KOH after washing with water) exhibited a significantly higher adsorption capacity of 740.7 mg/g. ACG-4b (KOH-activated after washing with NaOH) had a lower capacity of 549.5 mg/g. Our research revealed that the specific surface area of the adsorbents using CGs was significantly larger compared to existing adsorbents. This wide surface area has a notable impact on the maximum adsorption capacity and initial adsorption rate of the CG-derived adsorbents. These results can lead to the development of sustainable and cost-effective ACGs adsorbents for mitigating antibiotic contamination of water sources.

EXPERIMENTAL

1. Preparation of ACG from CG

Waste CGs, derived exclusively from Brazilian beans, were acquired from Paik's Café after roasting and brewing. A washing method utilizing 0.1 M NaOH and deionized (DI) water was employed to remove the brown color and any lingering organics. The CGs were washed five times using two different methods. After washing, the CGs were soaked in distilled water for 24 h. This prolonged soaking aided in the further elimination of any remaining residues, impurities, or unwanted organics from the CGs. The cleaned CGs were dried in an oven at 60 °C for one day. Subsequently, the dried CGs were carbonized by heating them at 700 °C for 1 h in a N_2 atmosphere. The carbonized CGs were combined with KOH in different mass ratios (CG : KOH=1 : 1, 1 : 2, 1 : 3, and 1 : 4 for ACG-1, ACG-2, ACG-3, and ACG-4, respectively). Subsequently, they were activated in the N_2 atmosphere at 700 °C for 2 h. Following activation, the ACGs were washed using a 2% HCl solution. After washing, the ACGs were dried in an oven at 60 °C for one day to remove any remaining moisture.

2. Isotherm and Kinetic Studies

AMX ($C_{16}H_{19}N_3O_5S$) was obtained from Sigma-Aldrich, and a working solution with a concentration range of 1-150 mg/L was prepared using DI water. The equilibrium concentration of AMX was maintained within the range of 15-120 mg/L. Approximately 0.01 g of ACGs was added to 100 mL of a solution with a predetermined concentration of AMX prepared using DI water. The mixture was stirred at room temperature for 24 h. Subsequently, the samples were filtered, and the adsorption capacities were calculated by comparing the initial and final concentrations.

To investigate the relationship between the initial concentrations (C_o) of AMX and the adsorbent, the adsorption ratios were tested at various C_o concentrations (i.e., 15, 30, 45, 60, 75, 90, 105, and 120 mg/L) over specific time periods. Different isotherms, including the Freundlich, Langmuir, and adsorption densities, were examined to establish the optimal correlation with the equilibrium curves. The Langmuir equation was utilized to calculate the maximum uptake capacity. To investigate the kinetics of the process, the removal rate of AMX (at a concentration of 75 mg/L) by the ACGs was measured at different time intervals, following the same procedure as described previously. The rate constants were determined using conventional rate expressions, such as the pseudo-second-order equation proposed by Ho [16].

3. Characterization

The change in mass of the CGs with temperature was investigated using derivative thermal gravimetry (DTG, DTG-60H, Shimadzu), as part of the thermal gravimetric analysis (TGA). Scanning electron microscopy (SEM; SNE-3000M, SEC) was used to examine the surface morphology of the samples. The surface areas of the samples were determined by analyzing the N_2 adsorption/desorption isotherms using a Micromeritics 3Flex analyzer (Micromeritics). Additionally, a spectrometer (UV-1800, Shimadzu) was used to obtain the UV-vis absorbance spectra of AMX in the aqueous phase.

RESULTS AND DISCUSSION

1. Characterization of ACG

The waste CGs underwent carbonization via thermal decomposition in nitrogen. Their surfaces were activated by KOH treatment. This continuous process produced ACGs with high specific surface areas and open textural porosity. These physical properties make ACGs suitable for adsorbing AMX onto their micropore surfaces. The specific surface area of an adsorbent is influenced by the thermal decomposition temperature. Therefore, as depicted in Fig. 1, the optimal thermal decomposition temperature was determined using TGA and DTG. Despite thorough drying of the CGs in a vacuum oven, a small quantity of water confined within the pores was eliminated within temperatures range of 25-200 °C. At approximately 250-350 °C, a mass loss of 60 wt% of the CGs was observed, likely due to the production of heavy hydrocarbons (tar) and gaseous substances resulting from the degradation of lignocellulose [17]. Tar evolution was observed to occur above 500 °C, whereas weight loss continued steadily from 500 to 850 °C, resulting in char consolidation. In the DTG analysis, a plateau region

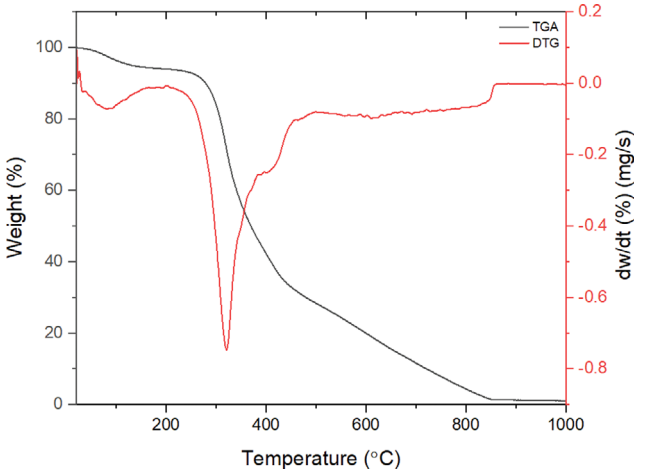

Fig. 1. Thermogravimetric analysis (TGA) curve (black) and DTG curve (red) for waste coffee grounds (CGs) in an N_2 atmosphere.

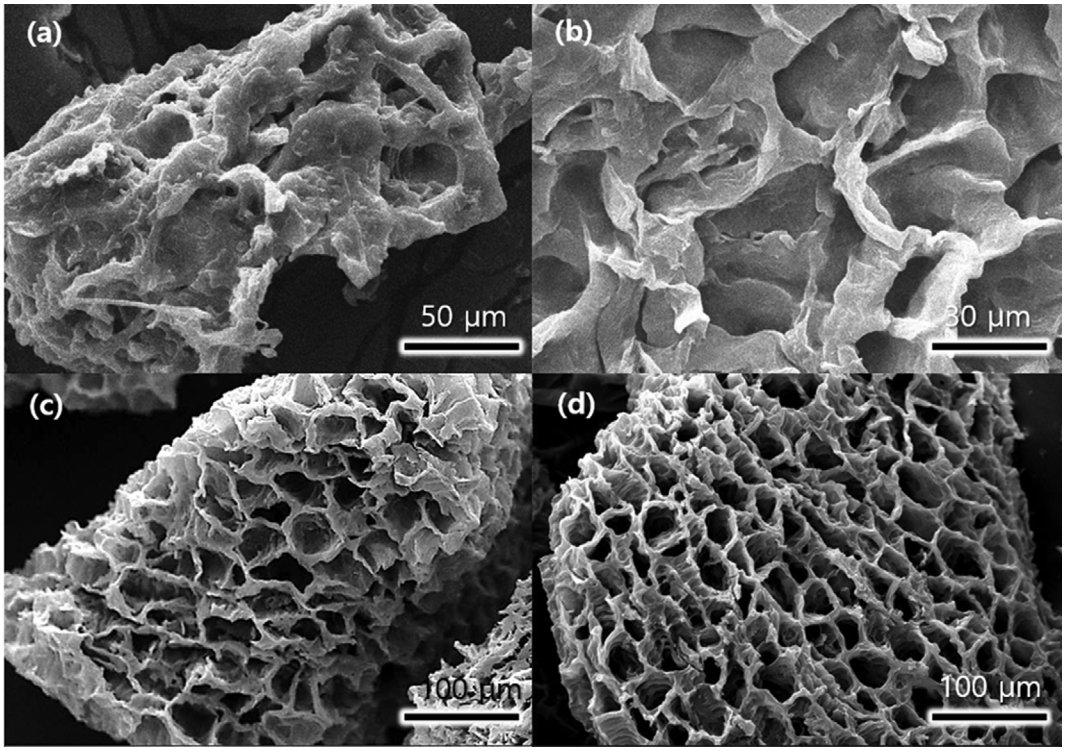

Fig. 2. Scanning electron microscopy (SEM) images of (a) CG, (b) CG after sequential water washing and carbonization, and activated coffee grounds (ACGs) after sequential (c) water and (d) NaOH washing, and carbonization and activation through KOH treatment.

was observed above 500 °C, indicating the carbonization progression. Consequently, ACGs formed below 500 °C did not exhibit char consolidation, whereas the desired biochar was formed above 500 °C. The high-temperature generation of non-carbon gases led to the development of an irregular open and texturally porous structure, producing a rigid carbon skeleton and facilitating the formation of micropores [18,19]. Based on these results, a thermal decomposition temperature of 700 °C was selected.

SEM analysis was conducted to observe changes in the surface morphologies of the CGs and ACGs after performing the two washing methods and activation through the KOH treatment (Fig. 2). The washed CGs did not contain visible macropores and had irregular surface morphology (Fig. 2(a)). After washing and carbonization, certain macropores of the CGs were blocked and clogged by residual carbon (Fig. 2(b)). Therefore, additional thermal or chemical treatments would be required to achieve a smooth surface with a clean textural porosity. Conversely, the ACGs that underwent carbonization and activation formed sponge-like macropores [20], regardless of the washing method employed (Figs. 2(c) and 2(d)). The gaseous substances generated during the carbonization process formed distinct pores as they exited the CGs. These pores contributed to the formation of macropores in the resulting ACGs.

KOH is used to activate carbonized biochar because of its ability to enhance the porous structure and surface properties of the material [8,13]. The activation process involves treating the carbonized biochar with KOH at elevated temperatures [21]. Through this process, KOH reacts with carbonized biochar, leading to the formation of pores and an increased surface area [9,15]. This development is advantageous for adsorption processes, as it enhances the binding sites for molecules and improves the overall adsorption capacity of the material. Additionally, KOH activation can modify the chemical composition of biochar [22], thereby enhancing its adsorption property for specific contaminants or target substances. The presence of KOH during the activation process can trigger the generation of active functional groups on the surface of the material [23], further enhancing its adsorption capability. The amount of gas generated during this thermal decomposition stage varies with the KOH mass ratio. This, in turn, can influence the formation of micropores and change the specific surface area of the resulting ACGs.

The pyrolysis of KOH produces K_2O, K_2CO_3, H_2O and other substances [24]. At high temperatures, these compounds react with carbon-based materials and generate CO and H_2. The porous structure of ACGs is formed through processes such as steam reforming reactions between water vapor and carbon, or the combination of K_2CO_3 with carbon, leading to the liberation of CO [25]. This leads to the removal of carbon atoms and formation of voids or pores within the material. The primary effect of KOH activation is the formation of wormhole-like micropores on the backbone of the ACGs [25]. The presence of micropores in the ACGs results in an increased specific surface area, thereby enhancing the maximum adsorption capacity of the adsorbent. Consequently, this synergistic effect is observed in ACGs with a combination of macropores and micropores, where the macropores facilitate the mobility of adsorbates and the micropores provide a large surface area for adsorption [26].

To verify the presence of micropores in the backbones of the ACGs, N_2 adsorption/desorption isotherm experiments were also

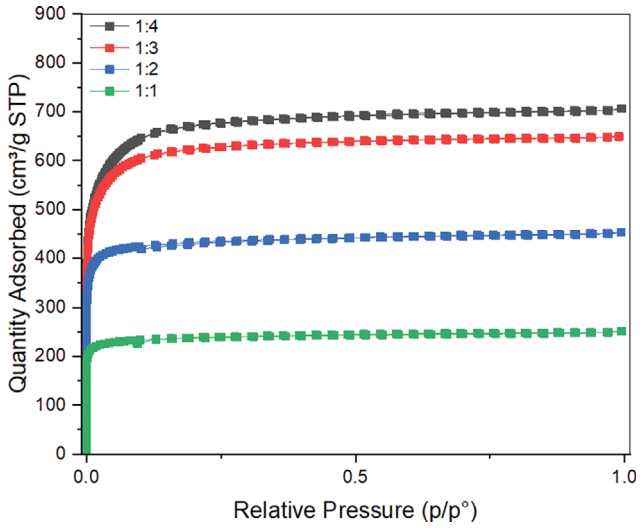

Fig. 3. N_2 adsorption/desorption isotherms of ACGs, which were prepared by different mass ratios of CG : KOH (1 : 1, 1 : 2, 1 : 3, and 1 : 4) after H_2O washing.

performed (Fig. 3). Table 1 summarizes the pore sizes and specific surface areas of ACG samples. Irrespective of the washing method employed (water or NaOH), the adsorption isotherm exhibited a typical type-I shape according to the IUPAC classification [27]. This type of isotherm is characteristic of microporous adsorbents and indicates the presence of micropores in the ACGs. The rapid increase in the adsorption curve at low pressures suggests the formation of narrow micropores [28]. As the content of KOH increased, the specific surface area of ACGs gradually increased, whereas the pore size remained generally similar, ranging from 30 to 25 Å. This observation suggests that a higher KOH content results in the generation of more gas during the thermal decomposition process, which increases the specific surface area by making the ACGs more porous. A study reported that the long and short axes and the molecular thickness of AMX were 9.30, 7.25, and 4.23 Å, respectively [29]. This indicates that the ACG samples possessed a significant degree

Table 1. Surface area and pore size of activated coffee ground (ACG) samples prepared by washing with NaOH and H_2O

Samples	Washing	Surface area (m^2/g)	Pore size (Å)[a]
ACG-1a	H_2O	937	30.1
ACG-2a		1,705	28.5
ACG-3a		2,376	25.6
ACG-4a		2,519	25.8
ACG-1b	NaOH	968	30.4
ACG-2b		1,680	32.3
ACG-3b		1,990	27.8
ACG-4b		2,345	24.6

[a]Micropore size was determined from the desorption average pore diameter (4 V/A).

of microporosity, which contributed to the high adsorption capacity of AMX. ACGs-4 exhibited a specific surface area approximately 2.5 times larger than that of ACGs-1, irrespective of the washing method employed. Interestingly, washing with water resulted in a marginally higher specific surface area than washing with NaOH. This finding suggests the practicality of using a non-toxic washing method to achieve favorable adsorbent properties. Consequently, ACGs-4, which was prepared through water washing with a CG : KOH ratio of 1 : 4, was selected for subsequent AMX adsorption and kinetics experiments.

2. Isotherm Studies

AMX is a representative antibiotic containing several functional groups (NH_2, OH, and COOH) in its molecular structure [30]. ACG has a high affinity for molecules containing amine groups (-NH_2) because of its ability to form strong interactions, such as hydrogen bonding and van der Waals forces. The amine group present in AMX facilitates effective adsorption onto the surface of ACGs through these interactions. The adsorption experiments employed ACGs-4 as the adsorbent, and the analysis involved the utilization of various isotherm equations (Table 2). The maximum adsorption capacity and binding energy were evaluated [31].

Table 2. Isotherms and kinetics equations used in this study [25]

Isotherms/kinetics	Equations	Remarks
Freundlich	$Q_e = K_F C_e^{1/n}$	C_e: equilibrium concentration of adsorbate Q_e: equilibrium concentration on the adsorbent K_F: Freundlich adsorption capacity n: Freundlich exponent
Langmuir	$Q_e = \frac{Q_m K_L C_e}{1 + K_L C_e}$	K_L: Langmuir adsorption capacity Q_m: maximum adsorption capacity
Adsorption density	$\Gamma_{max} = \frac{(C_i - C_e)V}{mS} \times 10^{-3}$	C_i: initial concentration of adsorbate V: volume of solution S: surface area of adsorbent m: amount of adsorbent
Pseudo-second-order	$\frac{t}{Q_t} = \frac{1}{k_{ad} Q_e^2} + \frac{t}{Q_e} = \frac{1}{h} + \frac{t}{Q_e}$	Q_t: adsorption capacity of adsorbent at time t k_{ad}: rate constant of adsorption t: time h: initial sorption rate

Table 3. Key constants of isotherm and kinetics equation for AMX adsorption by ACGs

Constants	H_2O washing				NaOH washing			
	ACG-1a	ACG-2a	ACG-3a	ACG-4a	ACG-1b	ACG-2b	ACG-3b	ACG-4b
Freundlich								
K_F (mg/g)	68.41	419.4	324.6	414.0	323.4	366.5	215.8	80.90
R^2	0.0005	0.0168	0.9228	0.5289	0.8118	0.1910	0.5741	0.6685
Langmuir								
Q_m (mg/g)	75.76	389.1	628.9	740.7	26.47	280.9	492.6	549.5
R^2	0.9687	0.9978	0.9953	0.9821	0.9657	0.9758	0.9965	0.9977
Adsorption density								
Γ_{max} (mol/m^2)	3.20×10^{-7}	7.19×10^{-7}	7.18×10^{-7}	8.73×10^{-7}	1.31×10^{-7}	5.13×10^{-7}	7.12×10^{-7}	6.52×10^{-7}
Kinetics								
h (mg/g·min)	3.82	5.63	8.56	9.02	5.56	6.00	6.28	7.77
k_{ad} (g/mg·min)	2.84×10^{-4}	8.08×10^{-5}	2.25×10^{-5}	2.70×10^{-5}	4.09×10^{-4}	1.22×10^{-4}	3.44×10^{-5}	3.33×10^{-5}

We expected a difference in the maximum adsorption capacities of the adsorbents because of the difference in pore characteristics (Table 1) caused by washing the ACGs with water and NaOH. As summarized in Table 3, the uptake capacity of AMX by ACGs-x varies with the sample type. The Freundlich isotherm was used to determine the adsorption capacity; however, the R^2 value, which indicates the goodness of fit of the equation to the data, was not adequately high. However, for the Langmuir isotherm, the R^2 values were generally greater than 0.96, indicating a good fit. The Langmuir theory assumes that the adsorption process occurs at specific uniform sites on the adsorbent surface, whereas the Freundlich isotherm assumes a surface with a non-uniform distribution of adsorption energy [32]. The Langmuir equation providing a better fit to the experimental data than the Freundlich equation suggests that the interaction between AMX molecules and the adsorbents is through chemisorption rather than physisorption. This implies that the adsorption of AMX onto the adsorbent surface involved stronger chemical bonding rather than only weak physical interactions. The linearity observed in the C_e (equilibrium concentration) vs. Q_e (amount adsorbed at equilibrium) graph (Fig. 4) indicates that the adsorption experiment corroborates the Langmuir isotherm. Notably, the adsorption process occurred at specific uniform sites on the surface of the adsorbent.

The maximum uptake capacity (Q_m) of ACGs increased from ACG-1 to ACG-4, with ACG-4a (washed with water and KOH-activated), exhibiting nearly ten times greater adsorption capacity (740.7 mg/g) than that of ACG-1a (75.76 mg/g). Conversely, the maximum adsorption capacity of ACG-4b (KOH-activated after washing with NaOH) was lower than that of ACG-4a after washing with water. These findings suggest that ACGs produced through water washing are not only more environmentally friendly but also demonstrate superior porosity and adsorption performance.

The adsorption density of the adsorbate per unit area was calculated using the formula in Table 2 considering the surface area of the adsorbent. As summarized in Table 3, the maximum adsorption density (Γ_{max}) generally exhibited a value of approximately 10^{-7} mol/m^2, and the adsorption density increased with higher ratios of KOH used for activation. This phenomenon can be attributed to the influence of KOH in improving the porous structure and surface properties of the ACGs. The activation process involves the

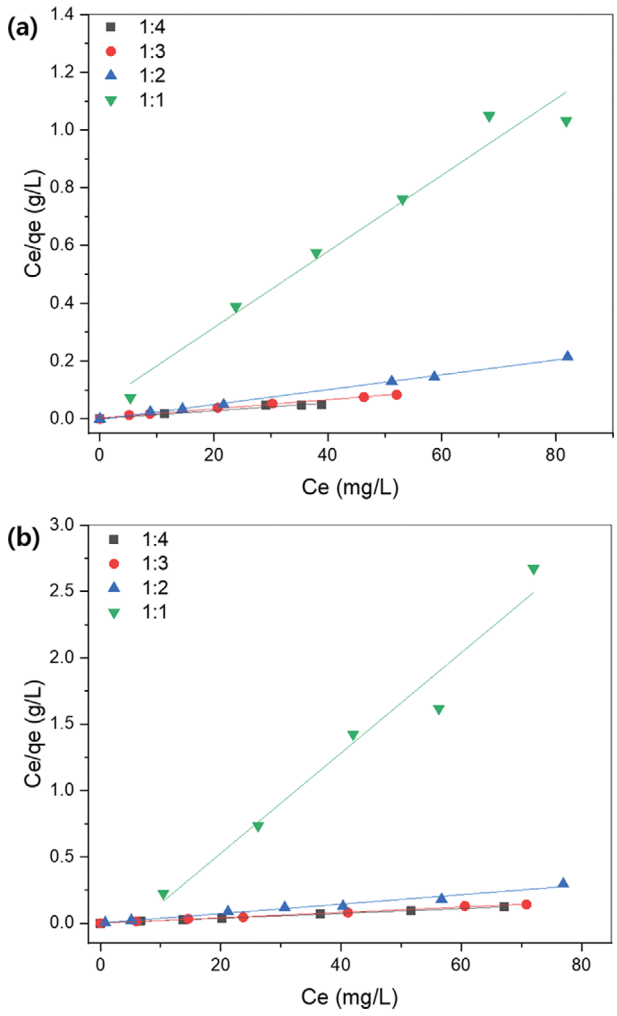

Fig. 4. Langmuir isotherm for amoxicillin (AMX) adsorption using ACGs prepared with different CGs : KOH activation ratios: (a) water and (b) NaOH washing.

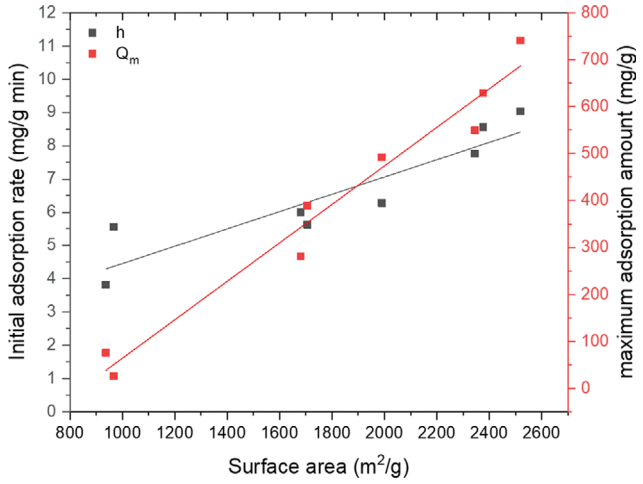

Fig. 5. Dependence of the maximum adsorption capacity and initial sorption rate with the surface area of ACGs.

reaction between KOH and carbonized biochar, leading to the pore formation and an increase in surface area. The enlarged surface area offers a greater number of adsorption sites, resulting in a higher adsorption density. Furthermore, KOH activation induces changes in the chemical composition of biochar, leading to the formation of active functional groups on the surface, which further enhances the adsorption capabilities of ACGs. Consequently, a higher KOH ratio contributes to an increased surface area and a greater number of active sites [33], leading to a higher adsorption density.

The adsorption density of the ACGs sample washed with water was higher than that washed with NaOH. This difference can be attributed to the influence of the washing method on the surface characteristics of ACGs. Water washing, which is a toxic-chemical-free method, likely results in cleaner textural porosity and a smoother surface than NaOH washing. A cleaner surface with well-developed porosity provides more accessible adsorption sites and facilitates adsorption. However, NaOH washing has the potential to introduce surface modifications or residual effects that can affect the adsorption performance of ACGs. These effects may encompass alterations in the surface chemistry or the presence of residual NaOH, which in turn might affect the adsorption capacity or accessibility of the adsorption sites. Conversely, the ACG samples washed with water demonstrated a higher adsorption density, indicating superior porosity and adsorption performance compared with the ones washed with NaOH.

The observed increase in AMX uptake capacity in ACGs with higher KOH ratios and higher adsorption density in the water-washed samples can be attributed to the combined effects of the activation process and employed washing methods. These factors influence the porosity, surface properties, and accessibility of the adsorption sites on ACGs, ultimately affecting their adsorption performance (Fig. 5).

3. Sorption Kinetics

The kinetics of sorption play a crucial role in determining the efficiency of the sorption process by governing the rate at which the solute is taken up and the residence time of the sorption reac-

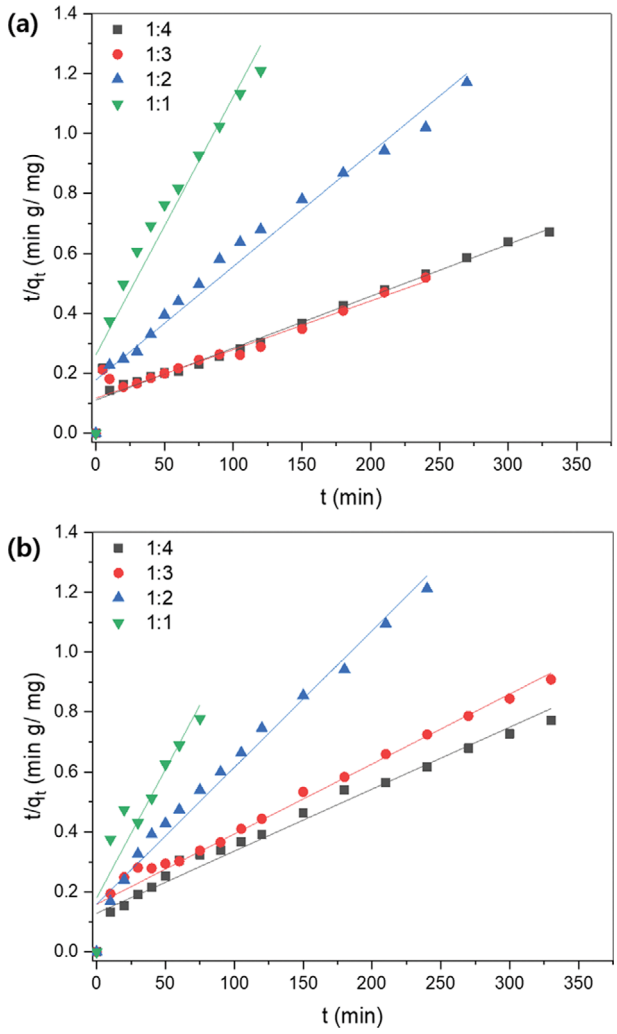

Fig. 6. Pseudo-second order kinetics for AMX adsorption using ACGs prepared with different CGs : KOH activation ratios: (a) water, and (b) NaOH washing.

tion. An appropriate kinetic model must be employed to understand changes in sorption over time. Traditionally, the pseudo-first-order Lagergren equation has been used to describe sorption kinetics [31]. However, in this study, we utilized a pseudo-second-order equation to describe the adsorption of AMX onto ACGs [16], as outlined in Table 2.

The initial sorption rate (h), equilibrium sorption capacity (q_e), and pseudo-second-order rate constant (k_{ad}) were experimentally determined by analyzing the graph of t/q_t vs. t (Fig. 6). Here, h is a function of time, indicating a time-dependent sorption process. The pseudo-second-order kinetic model exhibited a satisfactory fit for all concentrations, suggesting that the sorption reaction could be effectively approximated by this model. This equation offers a more comprehensive description of the sorption process by incorporating the chemisorption mechanism, involving stronger chemical bonding between the adsorbent (ACGs) and AMX molecules, rather than weak physical interactions. This model assumes that sorption occurs through a multistep adsorption process, where the rate-limiting step involves the sharing or exchange of electrons be-

Table 4. Comparison of reaction rates of different catalytic systems for amoxicillin (AMX) removal

Sample	Surface area (S, m^2/g)	Maximum uptake (Q_m, mg/g)	Adsorption rate (k_{ad}, g/mg·min)	References
Waste coffee	2,519	740	2.70×10^{-5}	This study
ZnO@carbon nanofiber	-	156	1.68×10^{-3}	[27]
Montmorillonite	34	648	5.00×10^{-5}	[28]
Shell powder	4.2	132	1.08×10^{-3}	[29]
Graphene nanoplatelet	543	106	2.35×10^{-2}	[30]
Bio-hydrochar	1,216	93	3.50×10^{-2}	[31]
Cellulose nanocomposite	76	114	4.18×10^{-2}	[32]

tween the adsorbent and adsorbate [34]. The satisfactory fit of the pseudo-second-order kinetics model for all concentrations suggests that the adsorption capacity of the ACGs was determined by the availability of active adsorption sites on the surface, rather than being limited by external mass transfer processes.

The h values of the ACGs were influenced by the degree of KOH activation, with higher activation resulting in higher initial adsorption rates. For instance, ACG-4a exhibited a higher initial adsorption rate (9.02 mg/g·min) than ACG-1a (3.82 mg/g·min). Additionally, the adsorbents washed with water, such as ACG-4b, exhibited superior performance with a higher initial adsorption rate (7.77 mg/g·min) than those washed with NaOH. This phenomenon can be attributed to the specific surface area of the adsorbent, as revealed by isothermal adsorption experiments. In Fig. 5, a general linear relationship can be observed between the h and S of the adsorbent. Surface area plays a crucial role in determining the availability of active adsorption sites and the extent of interaction between the adsorbate (AMX) and the adsorbent (ACGs).

Overall, a higher specific surface area enables a larger contact area between the two, facilitating more rapid and efficient adsorption. This increased surface area provides greater access to active adsorption sites, leading to enhanced adsorption kinetics and higher initial adsorption rates. Therefore, adsorbents with higher specific surface areas, achieved through higher KOH activation or water washing, exhibited improved performance in terms of initial adsorption rates.

To confirm the superiority of the AMX-adsorption performance of the ACG adsorbent, the maximum adsorption capacities and adsorption rates of various other adsorbents were compared (Table 4) [35-40]. Among the adsorbents examined, biochar exhibited relatively large surface areas [39], whereas graphene exhibited a significant surface area. Although montmorillonite had a higher maximum adsorption capacity of 648 mg/g despite its smaller surface area [36], it could not outperform the ACGs in terms of AMX-adsorbing capacity. Conversely, numerous adsorbents displayed adsorption rates of approximately 10^{-2} g/mg·min, indicating that the ACGs did not have a significant adsorption rate.

CONCLUSIONS

The employed ACG adsorbents exhibited exceptional characteristics, making them promising for use in the removal of antibiotics from water sources. The environmentally friendly nature of ACG adsorbents, achieved through water washing without the use of chemicals, highlights their potential for sustainable and eco-friendly use. Moreover, the ACG adsorbents demonstrated superior performance compared to previously reported adsorbents, exhibiting the highest AMX adsorption performance. The substantial surface area of biochar-based adsorbents, including ACGs, significantly contributes to their enhanced adsorption capacity. This attribute, coupled with its favorable adsorption performance, establishes its suitability for efficient removal of AMX from aqueous solutions. Although the ACGs may not possess the highest adsorption rates among the considered adsorbents, their overall performance in terms of the maximum adsorption capacity and eco-friendliness indicates that they are excellent candidates for AMX adsorption. Thus, they can help mitigate water pollution and safeguard aquatic ecosystems. Furthermore, their environment-friendly production process, which is free from chemical treatments, reduces the release of harmful substances into the environment. This aligns with the principles of sustainable development and highlights the importance of employing eco-friendly technologies for water remediation.

ACKNOWLEDGEMENTS

This study was funded by the National Research Foundation of Korea (grant number: NRF-2022R1F1A1059495).

REFERENCES

1. Ö. Kerkez-Kuyumcu, Ş. S. Bayazit and M. A. Salam, *J. Ind. Eng. Chem.*, **36**, 198 (2016).
2. Z. Zhang, Z. Xu and X. Wang, *Environ. Int.*, **176**, 107964 (2023).
3. M. Khalid, X. Liu, B. Zheng, L. Su, D. J. Kotze, H. Setälä, M. Ali, A. Rehman, S. U. Rahman and N. Hui, *J. Clean. Prod.*, **409**, 137275 (2023).
4. Q. Zheng, Y. Zhang, Q. Zhang, Y. Wang and G. Yu, *Chemosphere*, **319**, 138039 (2023).
5. S. Li, Y. Wu, H. Zheng, H. Li, Y. Zheng, J. Nan, J. Ma, D. Nagarajan and J. S. Chang, *Chemosphere*, **311**, 136977 (2023).
6. M. Zou, W. Tian, M. Chu, Z. Lu, B. Liu and D. Xu, *Sci. Total Environ.*, **879**, 163057 (2023).
7. M. Lv, F. Chen, Z. Zhang, D. Li, M. Hassan, Z. Gong and Y. Feng, *Sep. Purif. Technol.*, **315**, 123643 (2023).
8. J. Lee, S. Lee and Y. K. Park, *Bioresour. Technol.*, **385**, 129419 (2023).
9. P. Bhavani, M. Hussain and Y. K. Park, *J. Cleaner Prod.*, **330**, 129899 (2022).
10. A. Srivastava, H. Dave, B. Prasad, D. M. Maurya, M. Kumari, M.

Sillanpää and K. S. Prasad, *Inorg. Chem. Commun.*, **144**, 109895 (2022).
11. J. Roh, H. N. Umh, C. M. Yoo, S. Rengaraj, B. Lee and Y. Kim, *Korean J. Chem. Eng.*, **29**, 903 (2012).
12. L. L. Kang, Y. N. Zeng, Y. T. Wang, J. G. Li, F. P. Wang, Y. J. Wang, Q. Yu, X. M. Wang, R. Ji, D. Gao and Z. Fang, *J. Water Proc. Eng.*, **49**, 103178 (2022).
13. H. Laksaci, A. Khelifi, B. Belhamdi and M. Trari, *J. Environ. Chem. Eng.*, **5**, 5061 (2017).
14. M. Gurrath, T. Kuretzky, H. P. Boehm, L. B. Okhlopkova, A. S. Lisitsyn and V. A. Likholobov, *Carbon*, **38**, 1241 (2000).
15. C. H. Wang, W. C. Wen, H. C. Hsu and B. Y. Yao, *Adv. Powder Technol.*, **27**, 1387 (2016).
16. Y. S. Ho and G. McKay, *Water Res.*, **34**, 735 (2000).
17. W. Travis, S. Gadipelli and Z. Guo, *RCS Adv.*, **5**, 29558 (2015).
18. A. S. González, M. G. Plaza, J. J. Pis, F. Rubiera and C. Pevida, *Energy Procedia*, **37**, 134 (2013).
19. H. Laksaci, A. Khelifi, M. Trari and A. Addoun, *J. Clean. Prod.*, **147**, 254 (2017).
20. X. Liu, S. Zhang, X. Wen, X. Chen, Y. Wen, X. Shi and E. Mijowska, *Sci. Rep.*, **10**, 3518 (2020).
21. R. Nandi, M. K. Jha, S. K. Guchhait, D. Suttradhar and S. Yadav, *ACS Omega*, **8**, 4802 (2023).
22. F. Lü, X. Lu, S. Li, H. Zhang, L. Shao and P. He, *Chem. Eng. J.*, **429**, 132203 (2022).
23. P. Pinij, N. Tippayawong, Y. Chimupala and S. Chaiklangmuang, *J. Anal. Appl. Pyrolysis*, **157**, 105234 (2021).
24. E. Raymundo-Pinero, P. Azais, T. Cacciaguerra, D. Cazorla-Amoros, A. Linares-Solano and F. Beguin, *Carbon*, **43**, 786 (2005).
25. M. J. Kim, S. W. Choi, H. Kim, S. Mun and K. B. Lee, *Chem. Eng. J.*, **397**, 125404 (2020).
26. C. F. Wang, C. L. Wu, S. W. Kuo, W.-S. Hung, K. J. Lee, H. C. Tsai, C. J. Chang and J. Y. Lai, *Sci. Rep.*, **10**, 12769 (2020).
27. M. D. Donohue and G. L. Aranovich, *Adv. Colloid Interface Sci.*, **76-77**, 137 (1998).
28. X. Liu, C. Sun, H. Liu, W. H. Tan, W. Wang and C. Snape, *Chem. Eng. J.*, **361**, 199 (2019).
29. H. Nabipour, M. H. Sadr and N. Thomas, *J. Exp. Nanosci.*, **10**, 1269 (2015).
30. A. A. Aryee, R. Han and L. Qu, *J. Clean. Prod.*, **368**, 133140 (2022).
31. Y. Kim, C. Kim, I. Choi, S. Rengaraj and J. Yi, *Environ. Sci. Technol.*, **38**, 924 (2004).
32. J. D. Seader and E. J. Henley, *Separation process principles*, John Wiley, New York (1998).
33. S. Wang, Y. R. Lee, Y. Won, H. Kim, S. E. Jeong, B. W. Hwang, A. R. Cho, J. Y. Kim, Y. C. Park, H. Nam, D. H. Lee, H. Kim and S. H. Jo, *Chem. Eng. J.*, **437**, 135378 (2022).
34. J. C. Bullen, S. Saleesongsom, K. Gallagher and D. J. Weiss, *Langmuir*, **37**, 3189 (2021).
35. J. M. Chab and P. N. Nomngongo, *Emerg. Contam.*, **5**, 143 (2019).
36. J. Imanipoor, A. Ghafelebashi, M. Mohammadi, M. Dinari and M. R. Eshsani, *Colloids Surf. A Physicochem. Eng. Asp.*, **611**, 125792 (2021).
37. A. A. Mohammed, T. J. Al-Musawi, S. L. Kareem, M. Zarrabi and A. M. Al-Ma'abreh, *Arabian J. Chem.*, **13**, 4629 (2020).
38. Ö. Kerkez-Kuyumcu, S. S. Bayazit and M. A. Salam, *J. Ind. Eng. Chem.*, **36**, 198 (2016).
39. H. Li, J. Hu, Y. Cao, X. Li and X. Wang, *Bioresour. Technol.*, **246**, 168 (2017).
40. C. Yang, L. Wang, Y. Yu, P. Wu, F. Wang, S. Liu and X. Luo, *Int. J. Biol. Macromol.*, **149**, 93 (2020).